NASA Technical Paper 2375

June 1990

Transonic Flow Analysis for Rotors

Part 3—Three-Dimensional, Quasi-Steady, Euler Calculation

I-Chung Chang

NASA

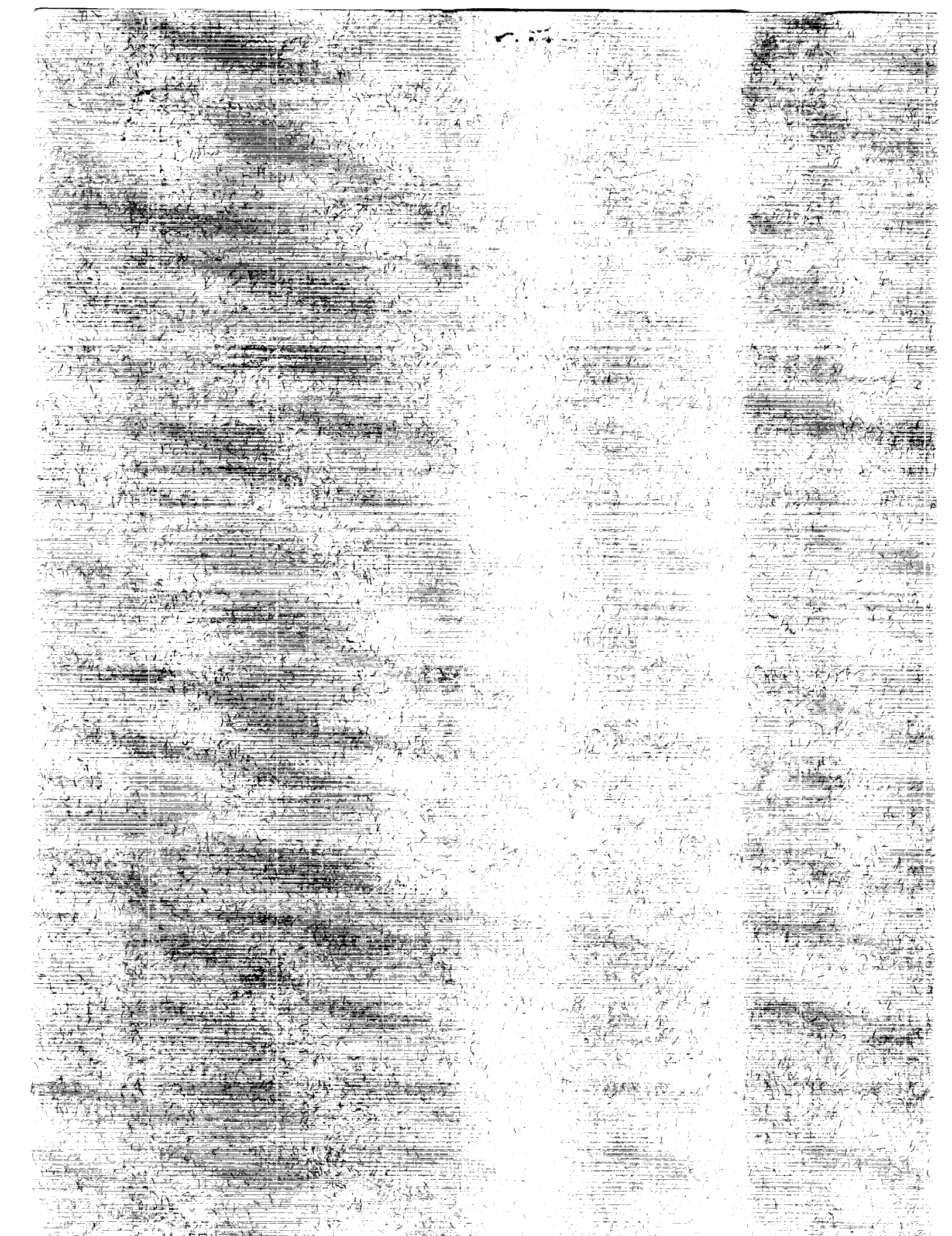

NASA Technical Paper 2375

1990

Transonic Flow Analysis for Rotors

Part 3—Three-Dimensional, Quasi-Steady, Euler Calculation

I-Chung Chang
Ames Research Center
Moffett Field, California

National Aeronautics and Space Administration
Office of Management
Scientific and Technical Information Division

SYMBOLS

c	local speed of sound
C_p	pressure coefficient
E	total energy
H	enthalpy
MACH	Mach number
M_T	maximum tip Mach number due to the rotation of rotor
p	pressure
q	absolute velocity in the inertial frame of reference
q_r	relative velocity in the rotor-fixed frame of reference
S	entropy
SMACH	sectional Mach number
U	forward flight velocity of the rotor
X/C	chordwise relative position on a profile
γ	ratio of specific heats
ν	advance ratio
Ω	angular velocity of the rotor
∂	partial differential operator
Ψ	blade azimuthal position
ρ	density
θ_c	collective pitch angle

SUMMARY

A new method is presented for calculating the quasi-steady transonic flow over a lifting or nonlifting rotor blade in both hover and forward flight by using Euler equations. The approach is to solve the Euler equations in a rotor-fixed frame of reference using a finite volume method. A computer program was developed and was then verified by comparison with wind-tunnel data. In all cases considered, good agreement was found with available experimental data.

INTRODUCTION

The computational prediction of aerodynamic forces on three-dimensional lifting rotor blades is the first step toward the computerized design of advanced rotors. It is apparent that computational methods will play a major role in the design and analysis of future rotary-wing vehicles (ref. 1). Several prediction methods (ranging from transonic small disturbance (refs. 2–3), through transonic full-potential (refs. 4–10), to Euler (refs. 11–12) techniques) for calculating transonic flow over a rotor blade have recently been proposed. However, the development of more accurate, efficient and robust methods will certainly continue until the viscous flow field around an entire rotorcraft can be economically calculated.

In this paper, a new solution method is described for the numerical solution of the Euler equations as applied to helicopter rotors. The method solves the three-dimensional Euler equations in a rotor-fixed frame of reference using a finite volume method. A computer program based on this method is designated as TFAR3 in the Transonic Flow Analysis for Rotors (TFAR) series of advanced computer codes developed at NASA Ames Research Center (refs. 5–6). The TFAR3 code can be used to calculate the flow past a lifting rotor, in both hover and forward flight, with the blade tip in a transonic flow regime. The geometry of the rotor blade can be quite general. The usual helicopter design parameters such as shaft angle, collective pitch angle, local twist angle, flapping angle, and variable tip shape are taken into account.

The TFAR3 code had been verified by comparison with wind-tunnel data (refs. 13–14). To establish the usefulness of the code, computational results are presented for the following cases in the hierarchy of flow-field complexity.

1. Nonlifting rotors in forward flight: computations were made for rotors with different blade tip shapes.

2. Lifting rotors in hover: several comparisons were made for a two-bladed model rotor in hover at different tip speeds.

3. Lifting rotors in forward flight: computations were made for a three-bladed lifting model rotor in forward flight.

In all the cases considered, good agreement was found with published experimental data.

This is Part 3 of a series of planned publications under the same general title "Transonic Flow Analysis for Rotors." The author would like to thank Dr. Frank Caradonna and

Dr. Chee Tung of the U. S. Army Aviation Research and Technology Activity, Aeroflightdynamics Directorate, for their critical and fruitful discussions and their generous assistance with the rotor wake modeling.

FLOW FIELD ANALYSIS PROBLEM

The rotor flow field is acknowledged to contain very complicated three-dimensional, unsteady, and viscous flow phenomena. During each revolution, the rotor blade may enter a transonic flow regime on the advancing side and may face boundary-layer separation on the retreating side. Moreover, the blade may encounter wakes shed from other blades with a complex blade-vortex interaction. Because of these complexities, the entire problem cannot be modeled with current computer capabilities. In this paper, we will focus on the advancing-blade side of the rotor flow field, particularly on the transonic effects.

While the potential flow solutions have proved extremely useful for transonic flows with shock waves of moderate strength, they are limited by an inherent inability to correctly predict stronger shock jumps. Also, the roll-up of the near wake and the convection of tip vortices are not easily modeled because a complex wake tracking is required. In this section we describe the flow field analysis problem in terms of Euler equations and discuss the boundary conditions at the outer computational boundaries.

Euler Equations in a Rotor-Fixed Reference Frame

Let the rotor-fixed frame of reference move with a constant linear velocity U and a constant angular velocity Ω with respect to an inertial frame of reference. The relative velocity V of a point fixed in the moving frame of reference is

$$V = U + \Omega \times r$$

where r is the position vector. Let the ambient density ρ_∞, speed of sound c_∞, and the reference chord length be unity. The nondimensional Euler equations in this rotor-fixed frame of reference are found to be

$$\begin{gathered} \rho_t + \nabla(\rho q_r) = 0 \\ (\rho q_r)_t + \nabla(\rho q_r q_r + p) + 2\rho\Omega \times q_r + \rho\Omega \times V + \rho V_t = 0 \\ (\rho E)_t + \nabla(\rho H q_r) + \rho(q_r + V)V_t = 0 \end{gathered} \tag{1}$$

where q_r is the velocity in the moving frame, ρ the density, p the pressure, E the total energy, and H the total enthalpy. The absolute velocity in the inertial frame of reference is given by $q = q_r + V$.

For a perfect gas,

$$E = \frac{p}{(\gamma - 1)\rho} + \frac{1}{2} q_r \cdot q_r - \frac{1}{2} V \cdot V$$

and

$$H = E + \frac{p}{\rho}$$

where γ is the ratio of the specific heats and is equal to 1.4 for air.

The tangential flow boundary condition on the rotor blade surface is

$$q_r \cdot n = 0$$

where n is the unit vector normal to the surface. At the outer computational boundaries, non-reflection boundary conditions as detailed in the next subsection are imposed.

Far-Field Boundary Condition

The boundary conditions at the far-field computational boundaries are derived by introducing Riemann invariants for one-dimensional flow normal to the boundaries.

The characteristic form of the one-dimensional Euler equations can be written as

$$\rho c[\partial_t + (q_r \cdot n \pm c)\partial_n](q \cdot n) \pm [\partial_t + (q_r \cdot n \pm c)\partial_n]p + \rho c(\Omega \times q \cdot n) = 0$$

$$[\partial_t + (q_r \cdot n)\partial_n]S = 0$$

where c is the speed of sound, n is the outward unit normal vector to the boundary, and S is the entropy.

For local isentropic flow, let a thermodynamic quantity $\sigma(\rho)$ be defined by

$$\sigma = \int \frac{dp}{\rho c}$$

then the first equation, after dividing through by ρc, is reduced to be

$$[\partial_t + (q_r \cdot n \pm c)\partial_n](q \cdot n \pm \sigma) + \Omega \times q \cdot n = 0$$

The quantities

$$R^{\pm} = q \cdot n \pm \sigma + \frac{\Omega \times q \cdot n}{q_r \cdot n \pm c}(r \cdot n)$$

which are called the Riemann invariants, are constant for the forward and backward characteristics. The invariants are propagated with speeds $q_r \cdot n \pm c$ along the characteristics respectively. Let subscripts ∞ and e denote the free-stream values and the values extrapolated from the interior adjacent to the boundary. For γ-law gas, considering subsonic flow, the free-stream and extrapolated Riemann invariants R_∞ and R_e at the outflow computational boundary are found to be

$$R_\infty = q_\infty \cdot n - \frac{2c_\infty}{\gamma - 1} + f$$

and

$$R_e = q_e \cdot n + \frac{2c_e}{\gamma - 1} + g$$

where f and g are given by

$$f = \frac{\Omega \times q_\infty \cdot n}{q_{r\infty} \cdot n - c_\infty}(r \cdot n)$$

and

$$g = \frac{\Omega \times q_e \cdot n}{q_{re} \cdot n + c_e}(r \cdot n)$$

correspondingly, and r is the position vector. These may be combined to give

$$q \cdot n = \frac{1}{2}(R_e + R_\infty - f - g)$$

and

$$c = \frac{(\gamma - 1)}{4}(R_e - R_\infty + f - g)$$

The quantities $q \cdot n$ and c are actually specified at the computational boundary. The other components of velocity are then extrapolated from the interior through the following formula

$$q = q_e + (q \cdot n - q_e \cdot n)n$$

The entropy S is also extrapolated from the interior $S = S_e$ for the outflow boundary. The density, energy and pressure can then be calculated from the entropy and the speed of sound. This procedure avoids specifying the pressure at the downstream boundary where it does not necessarily recover its free-stream value because of the trailing wake.

The conditions at the inflow, the inner radial and the outer radial computational boundaries can be derived in a similar manner.

For a computational region large enough to enclose the entire flow field about the whole rotor and its wake, the above boundary value problem is complete. For a computational region covering only a portion of the rotor disk, the flow effect caused by the other rotor blades and the flow outside the finite computational region have to be incorporated into the boundary conditions in some way. There are several methods of doing this. In the present work, this effect will simply be supplied by the inflow angle correction technique (refs. 7,15).

The quasi-steady problem is defined as the solution of the flow equations (1) with all the time derivative terms set equal to zero.

NUMERICAL SOLUTION PROCEDURE

Recently, efficient methods (refs. 16–19) for solving the Euler equations for steady flows have been developed for fixed-wing applications. Because the aim of this study is to develop a method for design work, the concern is for the easy applicability of the method to complex configurations. One possible approach to meet this need is the finite volume method. The Euler solver reported in references 19 and 20 has been adapted and modified for rotary-wing applications.

Finite Volume Scheme

The integral form of the Euler equation (1) can be written as

$$\partial_t \int\int\int_{vol} W d\tau + \int\int_{surf} F \cdot n ds + \int\int\int_{vol} G d\tau = 0 \tag{2}$$

Here, W is the conserved quantity, F the flux term, G the forcing term, $d\tau$ the volume element, ds the surface element, and n the outward unit normal vector.

The discretization procedure follows the method of lines in decoupling the approximation of the spacial and temporal terms. First, the computational domain in physical space is divided into hexahedral cells. Equation (2) is then approximated in each cell separately. Let the dependent variables be described at each center point (i, j, k) of the cells. A coupled set of ordinary differential equations is then obtained

$$\frac{d}{dt}(d\tau W) + Q + T = 0 \tag{3}$$

where Q is the flux term and T is the forcing term. The cell volume $d\tau$ can be determined as the sum of six tetrahedrons. Each of them can be evaluated by a simple formula as given in reference 21.

The flux term is given by

$$Q_{i,j,k} = \sum_{cellsides} F_{i,j,k} \cdot A_{i,j,k}$$

where $A_{i,j,k}$ denotes the area of the cell face between the points (i, j, k) and $(i + 1, j, k)$. The face area can be determined as one-half of the vector product of the cell face diagonals. The value of $F_{i,j,k}$ at the cell face is taken as the average of F at the points (i, j, k) and $(i + 1, j, k)$. The use of centered differences ensures the scheme of second order accuracy in spatial discretization, provided that the mesh is smooth enough.

At the blade surface, the only contribution to the flux balance comes from the pressure. The normal pressure gradient at the wall can be estimated in terms of quantities which can be determined from the interior solution as given in reference 22. The pressure on the blade is then estimated by extrapolation from the pressure at the adjacent cell centers.

Dissipative Terms

To inhibit odd/even point decoupling and to prevent the appearance of wiggles in the regions where pressure gradient is large, it is necessary to add artificial dissipative terms. Namely, equation (3) is replaced by

$$\frac{d}{dt}(d\tau W) + Q + T - D = 0 \tag{4}$$

where D is the dissipation term. An effective form for D is a blend of second and fourth order differences with coefficients depending upon the second order difference of the local pressure. Specifically, let ν be defined by

$$\nu_{i,j,k} = \frac{| p_{i+1,j,k} - 2p_{i,j,k} + p_{i-1,j,k} |}{p_{i+1,j,k} + 2p_{i,j,k} + p_{i-1,j,k}}$$

This quantity is second order except in regions containing a large pressure gradient. The term $D_{i,j,k}$ is constructed so that it is third order in smooth regions of flow and first order in the vicinity of the shock wave. $D_{i,j,k}$ has the form

$$D_{i,j,k} = (D_x + D_y + D_z)\omega_{i,j,k}$$

where ω is ρ for the continuity equation, ρq for the momentum equations, ρE for the energy equation, and D_x, D_y and D_z are central difference operators in i-, j- and k-directions respectively. Specifically, D_x is defined by

$$D_x\omega_{i,j,k} = d_{i+1/2,j,k} - d_{i-1/2,j,k}$$

$$d_{i+1/2,j,k} = \frac{d\tau_{i+1/2,j,k}}{\Delta t}[\epsilon^{(2)}_{i+1/2,j,k}\Delta_x\omega_{i,j,k} - \epsilon^{(4)}_{i+1/2,j,k}\Delta_x^3\omega_{i-1,j,k}]$$

and Δ_x is the forward difference operator given by

$$\Delta_x\omega_{i,j,k} = \omega_{i+1,j,k} - \omega_{i,j,k}$$

The coefficient

$$\epsilon^{(2)}_{i+1/2,j,k} = \kappa^{(2)} \cdot max(\nu_{i+1,j,k}, \nu_{i,j,k})$$

is made proportional to ν. The other coefficient is given by

$$\epsilon_{i+1/2,j,k} = max(0., \kappa^{(4)} - \epsilon^{(2)}_{i+1/2,j,k})$$

The fourth order differences provide background dissipation throughout the computational domain but are switched off in the neighborhood of the shock waves. The typical values of the constants $\kappa^{(2)}$ and $\kappa^{(4)}$ are 1/4 and 1/256.

Runge-Kutta Scheme

If the cell volume $d\tau$ is constant in time, the equation (4) has the form

$$W_t + R(W) = W_t + P(W) + D(W) = 0 \qquad (5)$$

where the residual $R(W)$ consists of convective part $P(W)$ and dissipative part $D(W)$. A class of Runge-Kutta four-stage time-stepping scheme can be employed to solve this system of ordinary differential equations. It can be written as

$$\begin{aligned} W^{(0)} &= W^n \\ W^{(1)} &= W^{(0)} - \alpha_1 \Delta t R^{(0)} \\ W^{(2)} &= W^{(0)} - \alpha_2 \Delta t R^{(1)} \\ W^{(3)} &= W^{(0)} - \alpha_3 \Delta t R^{(2)} \\ W^{(4)} &= W^{(0)} - \alpha_4 \Delta t R^{(3)} \\ W^{n+1} &= W^{(4)} \end{aligned} \tag{6}$$

where Δt is the time step, W^n and W^{n+1} the value of W at the beginning and end of the n-th time step, and in the (k+1)-th stage $R^{(k)} = P(W^{(k)}) + D(W^{(0)})$. The dissipation is evaluated once and then frozen after the first stage in each time step calculation. The choice of coefficients determines the characteristics of the scheme. For single grid calculations, a good choice of the coefficients is given by $\alpha_1 = .6$, $\alpha_2 = .6$, $\alpha_3 = 1.$, and $\alpha_4 = 1$.

Residual Smoothing

One way to extend the stability range of the explicit scheme is to perform the implicit residual smoothing. This process extends the domain of dependence and thus increases the stability range of the scheme.

The residual smoothing is applied in product form

$$(1 - \eta_i \partial_x^2) \cdot (1 - \eta_j \partial_y^2) \cdot (1 - \eta_k \partial_z^2) \overline{R}_{i,j,k} = R_{i,j,k}$$

where, $R_{i,j,k}$ is the residual before smoothing and $\overline{R}_{i,j,k}$ is the new residual. The coefficients are given by $\eta_i = 1$, $\eta_j = 1$, and $\eta_k = 1$. Because it is only necessary to solve a sequence of tridiagonal equations for scalar variables, this scheme requires a relatively small amount of computational effort per time step. Comparatively, other implicit schemes usually need to solve a coupling system with a much more costly block-tridiagonal solver. It is well known that a Runge-Kutta scheme with properly tuned residual smoothing can be shown to be unconditionally stable based on linear stability analysis (ref. 20). However, in practice, the fastest convergence to a steady state solution is realized with a small time step.

Local Time Stepping

For a steady state problem, the convergence of the scheme can be accelerated by using local time step. Namely, the solution advances in time with a time step size dictated by the local stability limit. This allows faster signal propagation on coarse mesh regions and thus faster convergence of the overall scheme. For single grid calculations, the use of local time step of Courant-Friedrichs-Lewy (CFL) number 4.0 gives rise to a good convergence rate for most cases.

Wake Modeling

For lifting rotor calculations, the wake effect and the blade motion are important. Because at present only a single blade of a rotor is contained in the finite domain of the computer code, a practical method is required to account for the far-field wake effect and other blade effects. A basic approach to solve this problem is to divide the entire flow field into two parts. The blade and its near wake will be modeled in the present code directly. The rest of the flow field which lies outside of the computational domain will be modeled through a set of inflow angles along the blade span at each azimuth position. This set of inflow angles can be furnished through auxiliary helicopter wake analysis codes. Two wake prediction codes are employed in the present study. For hover prediction, a linearized lifting surface code as reported in reference 23 is used. For forward flight prediction, a lifting line code as described in reference 24 is utilized. This technique was originally reported in reference 15 and had been employed in several recent papers (refs. 6, 8, 10).

RESULTS

Since only the coordinates in physical space of each grid point of the computational region are needed in the finite volume scheme, the body aligned mesh can be generated by several methods. The present computer code for a single rotor blade uses a simple C-type grid, which can be generated by a combination of stretching and conformal mappings similar to that in reference 5. Good solutions may be obtained by employing a grid of 129 points in streamwise, 33 points in normal, and 33 points in radial directions. The grid comprises 81 points on the airfoil surface and 21 points on the span of the rotor blade. A typical calculation needs about 600 time steppings to obtain a good solution and will take less than 15 min of CPU time on the Cray-XMP computer at Ames Research Center. For the same case, a multigrid calculation will take about 100 cycles to get a comparably accurate solution and will take about 5 min of CPU time on the same Cray-XMP computer.

The present calculations are mainly focused on transonic flows that occur on the advancing-blade side of a rotor in forward flight. All these studies have been performed with rigid blades in order to separate the aerodynamic and aeroelastic effects. A number of results are presented for the flow problems that are typically encountered in rotor flow calculations.

Nonlifting Rotors in Forward Flight

The first set of calculations is concerned with the fundamental case of nonlifting rotors for which there is no wake effect. Calculations were performed for model rotor blades with straight-tip and swept-back tip planforms. Figure 1 shows the planform of an ONERA nonlifting straight-tip model rotor blade (ref. 13). The surface pressure transducers are located at three spanwise stations of .855, .892, and .946. In figures 2a-d, the computed surface pressure distributions at these stations of the above blade are plotted and compared with ONERA measured data at an azimuth position ψ of 90^0 for moderate (0.4) to high (0.55) advance ratios μ. The tip Mach number M_T due to rotation for all the cases is 0.6. The results are quite satisfactory. Figure 3 shows the planform of the same ONERA model blade but with swept-back 30^0 blade tip. Figure 4 shows similar results for the model blade with this second blade tip at a tip Mach

number of 0.6288 and advance ratio of 0.5. The effect of this swept-back tip is clearly seen as a significant reduction of the suction peak over what occurs for a corresponding unswept case (fig. 2c).

Lifting Rotors in Hover

Calculations were made for a rigid two-bladed model rotor (ref. 14) in hover at various tip speeds. This model rotor employs an untapered NACA 0012 airfoil section and has an aspect ratio of 6. Calculations were performed for blades with a collective pitch angle θ_c of 8^0 and at three different tip Mach numbers of .612, .794, and .877. Here, the wake effects were calculated through a lifting surface code for hover prediction (ref. 23). Figures 5a-c show the comparison of calculated and measured surface pressure distributions at three spanwise stations of .80, .89, and .96 for the above three tip speeds. The overall agreement of surface pressure distributions is excellent for these three different cases. The locations of shock waves and the lower surface pressure distributions are predicted very well. The predictions of the surface pressure distributions at the inner two spanwise stations, 0.5 and .68 (which are not shown in this paper), are not as good as those at the outer spanwise stations. The disagreement may result from the presence of two vortex lines in the near field which are not currently taken into account.

Lifting Rotors in Forward Flight

For forward lifting flight calculation, the wake effects were obtained through a lifting line code (ref. 24). Computed results have been compared with experimental data for an ONERA three-bladed lifting model rotor at various high-speed forward flight conditions (ref. 13). Figure 6 shows the comparison of calculated and measured surface pressure distributions at three spanwise stations of .852, .902, and .951 near the blade tip. The azimuthal angle is 90^0. The tip Mach number is 0.6288 and the advance ratio μ is 0.3872. The overall agreement of surface pressure distributions is good. The discrepancies seen on the lower surface are presently not understood. However, similar comparisons have been found with other codes (refs. 6, 10).

CONCLUDING REMARKS

A new solution method for calculating the inviscid, rotational, quasi-steady transonic flow about helicopter rotors has been constructed. This method solves the conservation form of the Euler equations in a rotor-fixed frame of reference by a finite volume method. Based on this method, a three-dimensional Euler code was developed and validated. It has been shown that the code can be employed to calculate the flow past a lifting rotor in hover as well as in forward flight with the blade tip in a transonic flow regime. The geometry of the rotor blade can be quite general. A number of cases have been solved by using this new computer code, and the results were found to be accurate.

The tip vortex formation might be modeled by using this Euler code, and this possibility will be studied in the future. Other future works include incorporating a known vorticity field into the Euler calculation, and extending the current computer code to solve the Navier-Stokes equations for viscous flow calculations.

Ames Research Center
National Aeronautics and Space Administration
Moffett Field, California 94035-1000, January 26, 1990

REFERENCES

[1] Davis, S. S.; and Chang, I-Chung: The Critical Role of Computational Fluid Dynamics in Rotary-Wing Aerodynamics. AIAA Paper 86-0336, Jan. 1986.

[2] Caradonna, F. X.; and Isom, M. P.: Numerical Calculations of Unsteady Transonic Potential Flow over Helicopter Rotor Blades. AIAA Jnl., vol. 14, Apr. 1976, pp. 482-488.

[3] Chattot, J. J.: Calculation of Three-Dimensional Unsteady Transonic Flows Past Helicopter Blades. NASA TP-1721, 1980.

[4] Arieli, R.; and Tauber, M. E.: Computation of Subsonic and Transonic Flow about Lifting Rotor Blades. AIAA Paper 79-1667, Aug. 1979.

[5] Chang, I-Chung: Transonic Flow Analysis for Rotors - Part I. Three-Dimensional, Quasi-Steady, Full-Potential Calculation. NASA TP-2375, 1984.

[6] Chang, I-Chung: Transonic Flow Analysis for Rotors - Part II. Three-Dimensional, Unsteady, Full-Potential Calculation. NASA TP-2375, 1985.

[7] Chang, I-Chung; and Tung, C.: Numerical Solution of the Full-Potential Equation for Rotors and Oblique Wings Using a New Wake Model. AIAA Paper 85-0268, Jan. 1985.

[8] Tung, C.; and Chang, I-Chung: Rotor Transonic Computation with Wake Effect. Fourth International Conference on Applied Numerical Modeling, Taiwan, Rep. of China, Dec. 1984.

[9] Sankar, N. L.; and Prichard, D.: Solution of Transonic Flow Past Rotor Blades Using the Conservative Full-Potential Equation. AIAA Paper 85-5012, Oct. 1985.

[10] Strawn, R. C.; and Caradonna, F. X.: Numerical Modeling of Rotor Flows With a Conservative Form of the Full-Potential Equations. AIAA Paper 86-0079, Jan. 1986.

[11] Roberts, T. W.; and Murman, E. M.: Solution Method for a Hovering Helicopter Rotor Using the Euler Equations. AIAA Paper 85-0436, Jan. 1985.

[12] Sankar, N. L.; Wake, B. E.; and Lekoudis, S. G.: Solution of the Unsteady Euler Equations for Fixed and Rotor Wing Configurations. J. Aircraft, vol. 23, no. 4, Apr. 1986, pp. 283-289.

[13] Philippe, J. J.; and Chattot, J. J.: Experimental and Theoretical Studies on Helicopter Blade Tips at ONERA. ONERA TP 1980-96, Sep. 1980.

[14] Caradonna, F. X.; and Tung, C.: Experimental and Analytical Studies of a Model Helicopter Rotor in Hover. NASA TM-81232, Sep. 1981.

[15] Caradonna, F. X.; Desopper, A.; and Tung, C.: Finite-Difference Modeling of Rotor Flow Including Wake Effects. 8th European Rotorcraft Forum, Aix-en-Provence, France, Aug. 1982.

[16] Briley, W. R.; and MacDonald, H.: Solution of the Three Dimensional Compressible Navier-Stokes Equations by an Implicit Technique. Proc. 4th International Conference on Numerical Methods in Fluid Dynamics, 1974.

[17] Beam, R. M.; and Warming, R. F.: An Implicit Finite Difference Algorithm for Hyperbolic Systems in Conservation-Law Form. J. Comp. Phys., vol 22, no. 1, Sep. 1976, pp. 87-110.

[18] MacCormack, R. W.: A Numerical Method for Solving the Equations of Compressible Viscous Flow. AIAA Paper 81-110, Jan. 1981.

[19] Jameson, A.; Schmidt, W.; and Turkel, E.: Numerical Solution of the Euler Equations by Finite Volume Methods Using Runge-Kutta Time Stepping Schemes. AIAA Paper 81-1259, Jun. 1981.

[20] Jameson, A.; and Baker, T. J.: Solution of the Euler Equations for Complex Configurations. AIAA Paper 83-1929, Jul. 1983.

[21] Kordulla, W.; and Vinokur, M.: Efficient Computation of Volume in Flow Predictions. AIAA Jnl., vol. 21, no. 6, Jun. 1983, pp. 917-918.

[22] Rizzi, A.: Numerical Implementation of Solid Body Boundary Conditions for the Euler Equations. ZAMM, vol. 58, no. 7, Jul. 1978, pp.301-304.

[23] Summa, J.M.: Advanced Rotor Analysis Methods for the Aerodynamics of Vortex-Blade Interactions in Hover. Vertica, vol. 9, no. 4, 1985, pp. 331-343.

[24] Johnson, W.: Development of a Comprehensive Analysis for Rotorcraft 1. Rotor Model and Wake Analysis. Vertica, vol. 5, no. 2, 1981, pp. 99-129.

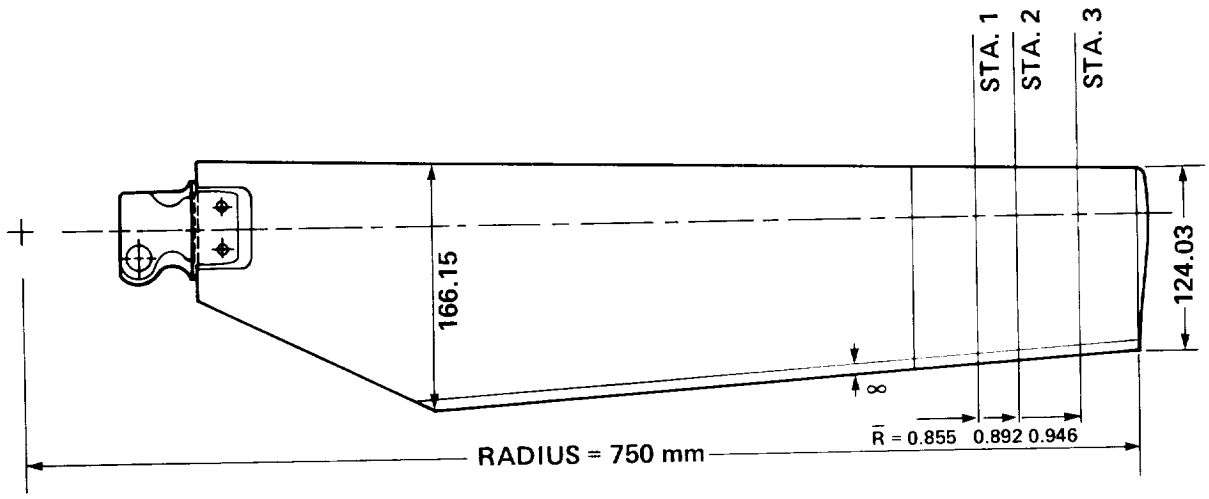

Figure 1. - Planform geometry of an ONERA nonlifting model rotor blade with straight tip.

$M_T = 0.6, \mu = 0.4, \psi = 90°$

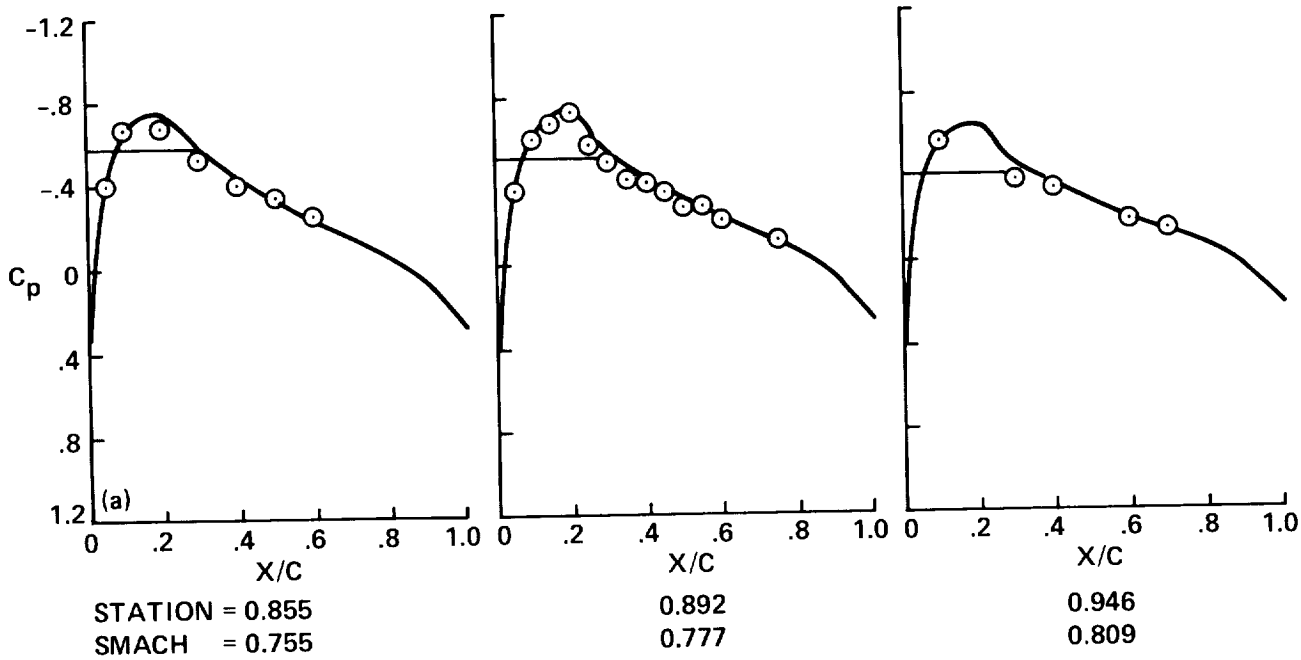

Figure 2. - Comparison of computed and measured surface pressure distributions for a nonlifting straight-tip blade in forward flight. (a) Advance ratio of .4.

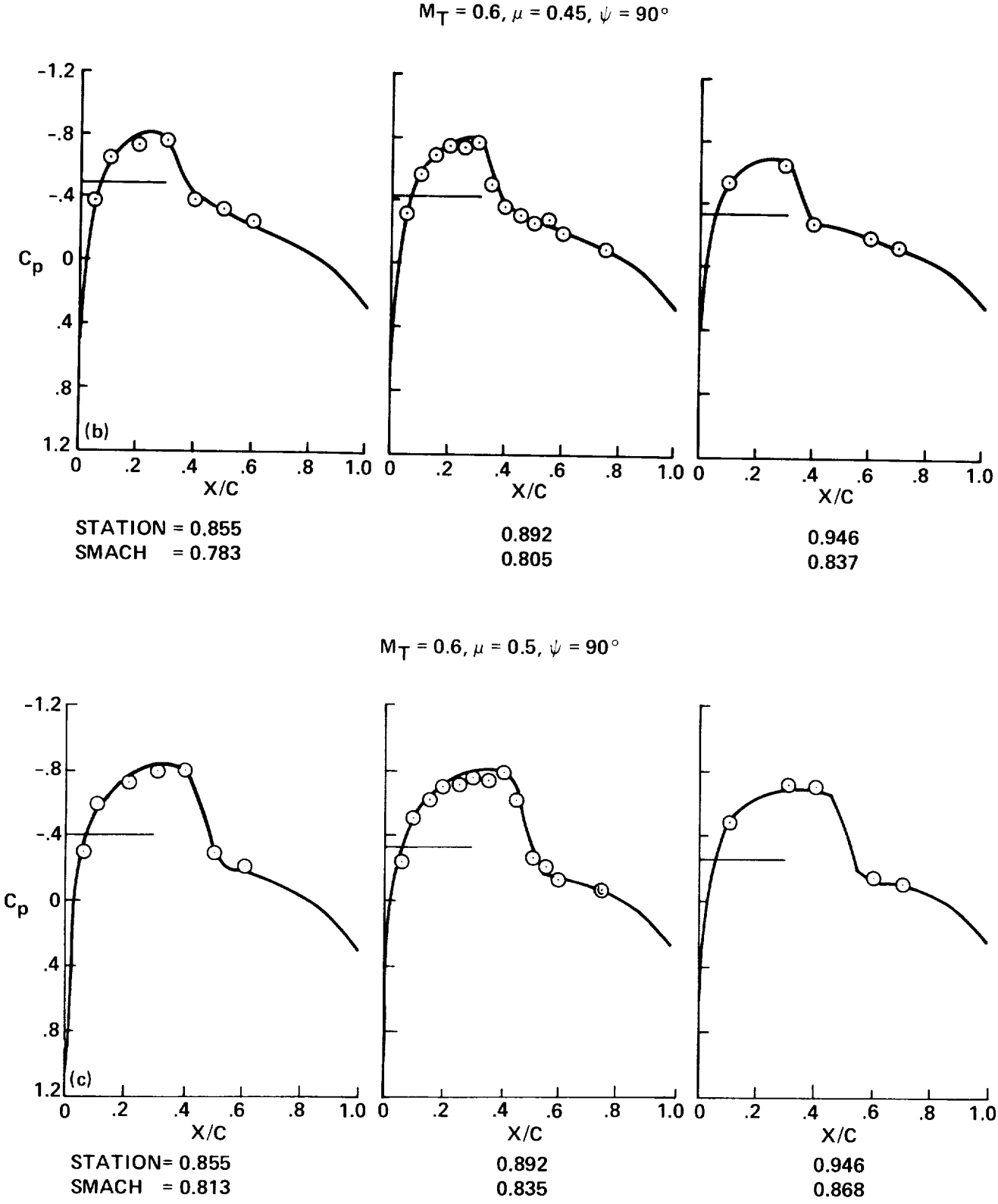

Figure 2. - Continued. (b) Advance ratio of .45. (c) Advance ratio of .5.

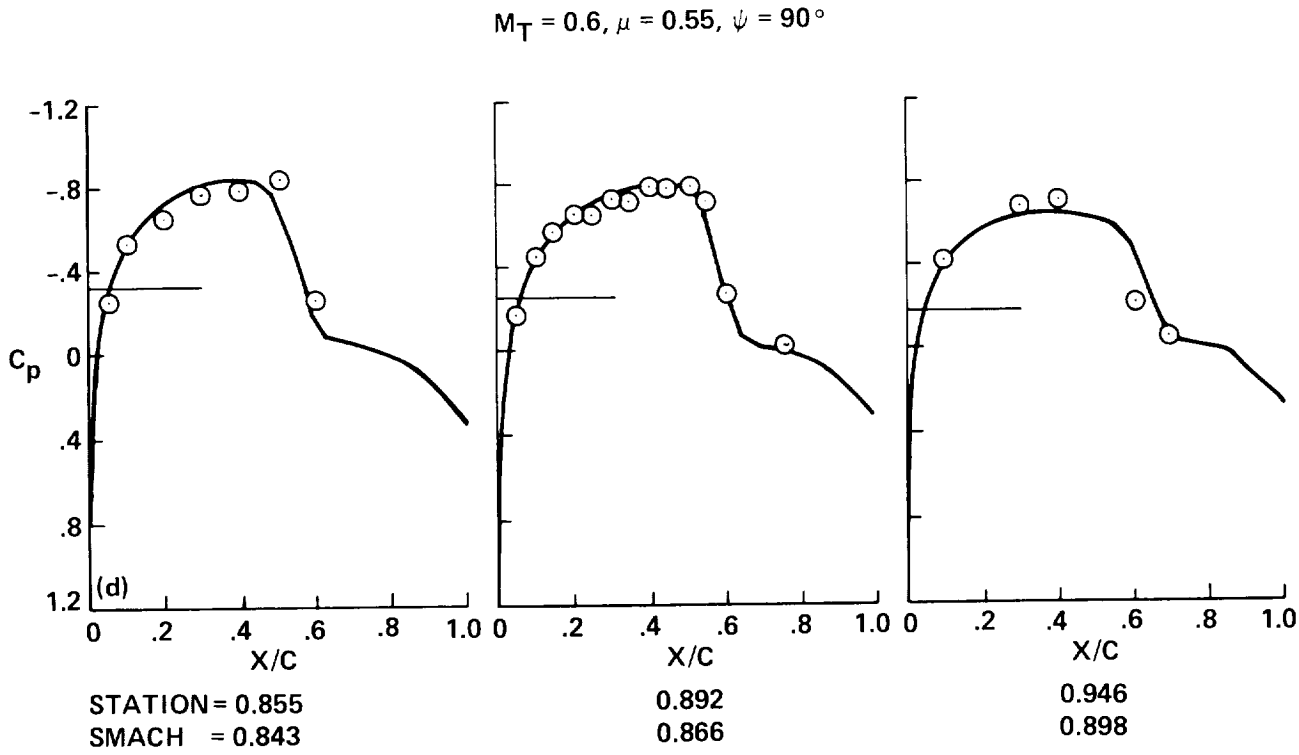

Figure 2. - Concluded. (d) Advance ratio of .55.

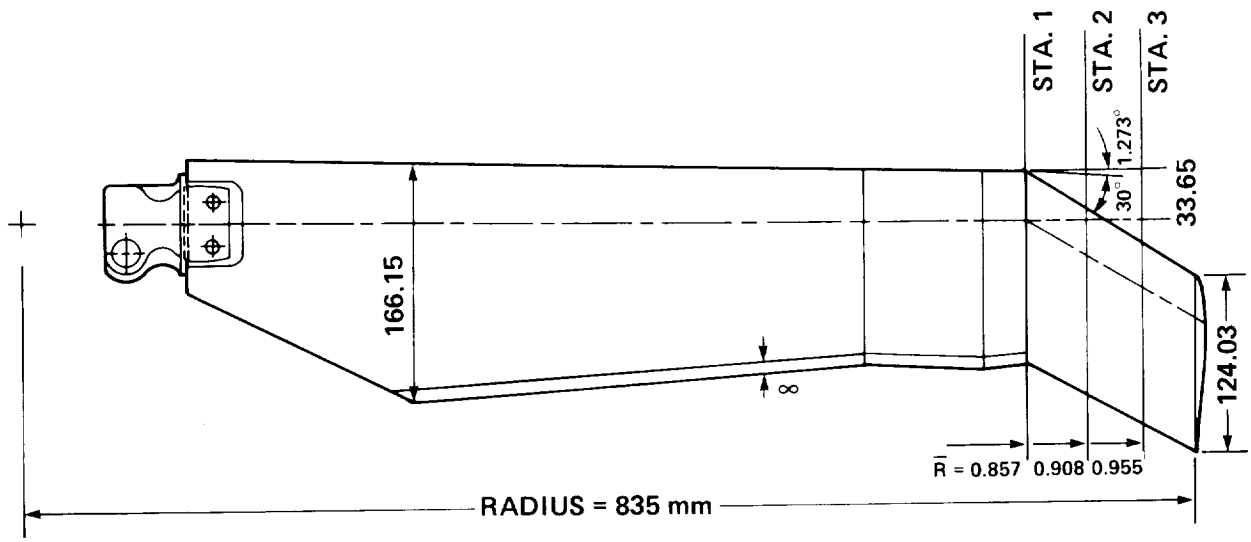

Figure 3. - Planform geometry of an ONERA nonlifting model rotor blade with swept-back 30^0 tip.

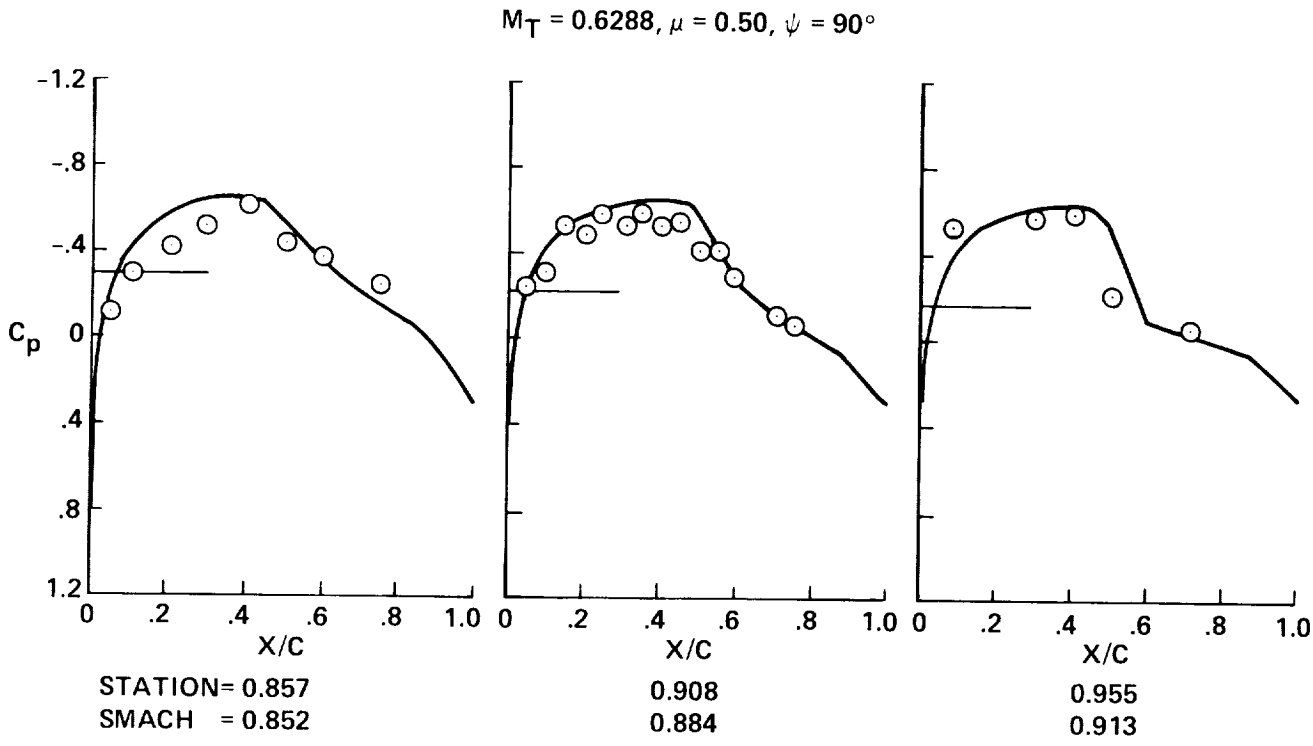

Figure 4. - Comparison of computed and measured surface pressure distributions for a nonlifting swept-back-tip blade in forward flight.

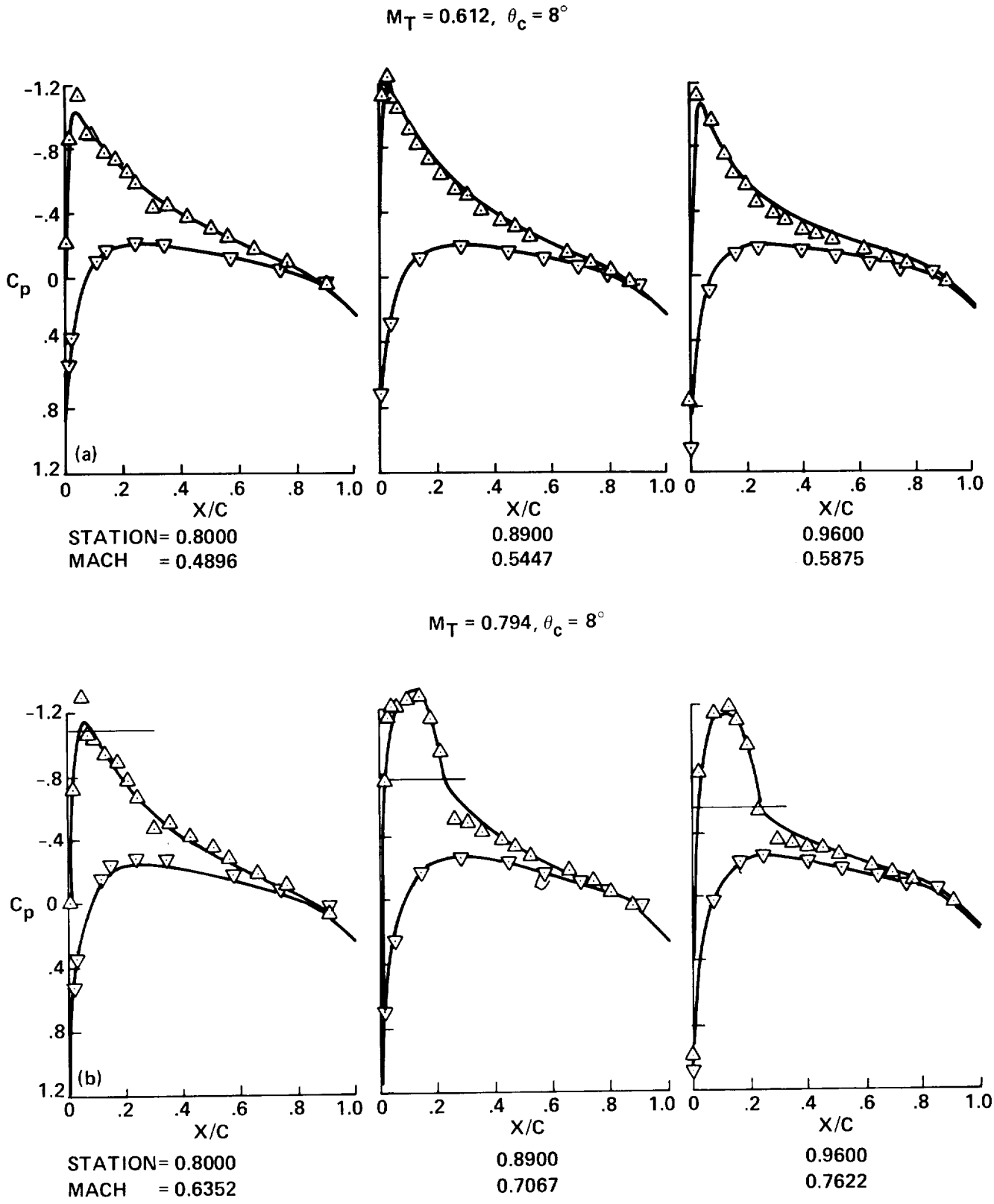

Figure 5. - Comparison of computed and measured surface pressure distributions for a lifting two-bladed rotor in hover. (a) Tip Mach number of .612. (b) Tip Mach number of .794.

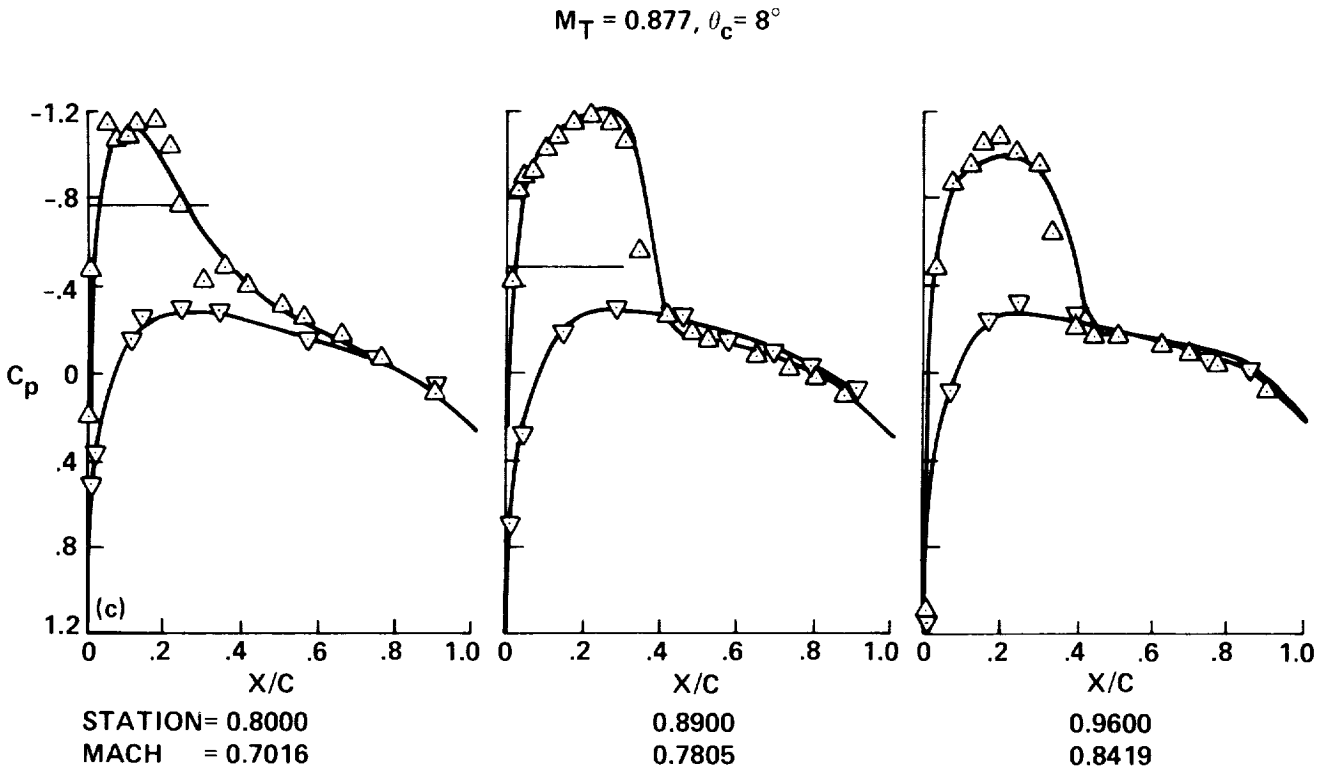

Figure 5. - Concluded. (c) Tip Mach number of .877.

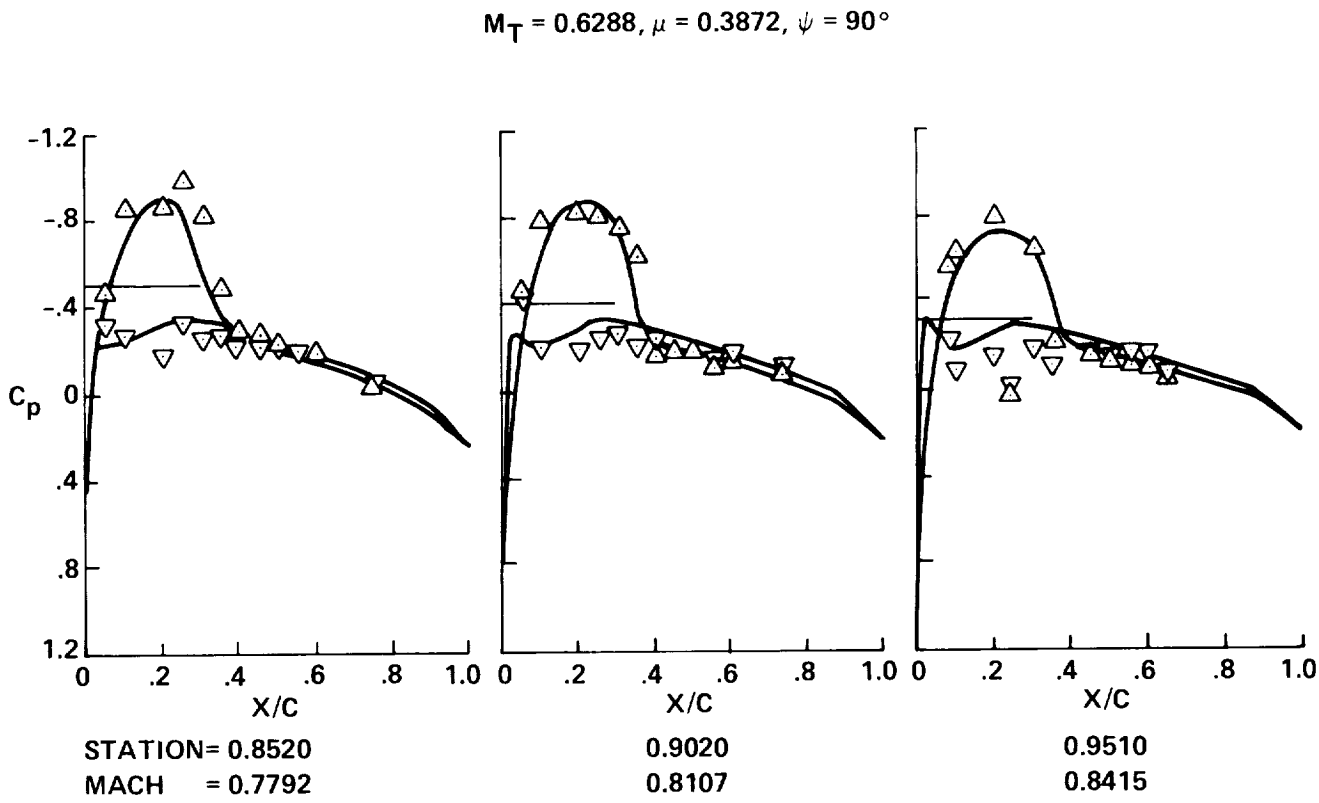

Figure 6. - Comparison of computed and measured surface pressure distributions for a lifting three-bladed rotor in forward flight.

NASA
National Aeronautics and Space Administration

Report Documentation Page

1. Report No.	2. Government Accession No.	3. Recipient's Catalog No.
NASA TP-2375		

4. Title and Subtitle

Transonic Flow Analysis for Rotors.
Part 3 – Three-Dimensional, Quasi-Steady, Euler Calculation

5. Report Date

June 1990

6. Performing Organization Code

7. Author(s)

I-Chung Chang

8. Performing Organization Report No.

A-86374

10. Work Unit No.

505-61-51

9. Performing Organization Name and Address

Ames Research Center
Moffett Field, CA 94035-1000

11. Contract or Grant No.

13. Type of Report and Period Covered

Technical Paper

12. Sponsoring Agency Name and Address

National Aeronautics and Space Administration
Washington, DC 20546-0001

14. Sponsoring Agency Code

15. Supplementary Notes

Point of Contact: I-Chung Chang, Ames Research Center, MS 260-1, Moffett Field, CA 94035-1000
(415) 604-6396 or FTS 464-6396

16. Abstract

A new method is presented for calculating the quasi-steady transonic flow over a lifting or nonlifting rotor blade in both hover and forward flight by using Euler equations. The approach is to solve Euler equations in a rotor-fixed frame of reference using a finite volume method. A computer program was developed and was then verified by comparison with wind-tunnel data. In all cases considered, good agreement was found with published experimental data.

17. Key Words (Suggested by Author(s))	18. Distribution Statement
Euler equations Transonic flow Rotor aerodynamics Finite volume method	Unclassified-Unlimited Subject Category - 02

19. Security Classif. (of this report)	20. Security Classif. (of this page)	21. No. of Pages	22. Price
Unclassified	Unclassified	24	A02

NASA FORM 1626 OCT 86

For sale by the National Technical Information Service, Springfield, Virginia 22161

NASA-Langley, 1990

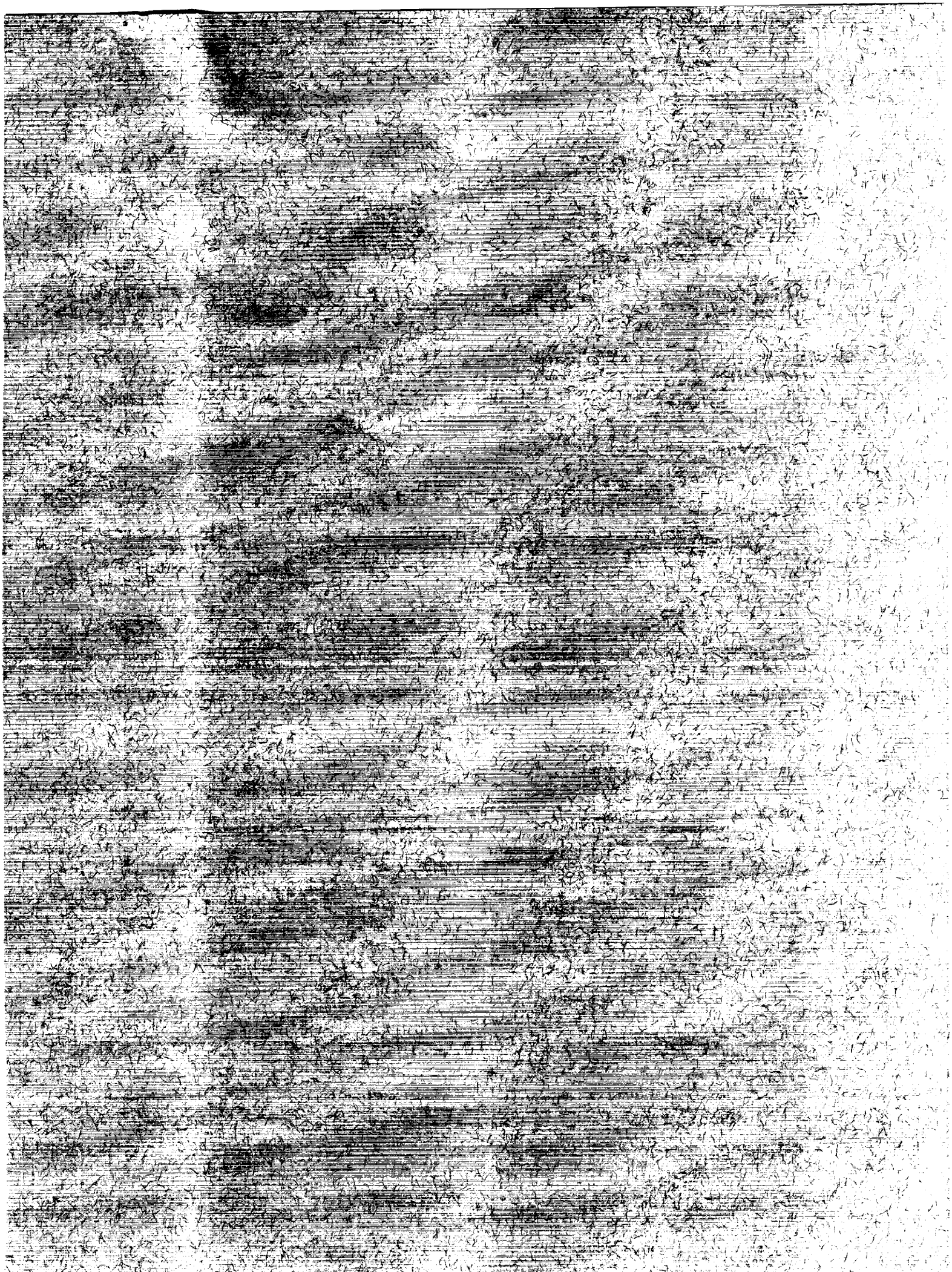

National Aeronautics and
Space Administration
Code NTT-4

Washington, D.C.
20546-0001

Official Business
Penalty for Private Use, $300

BULK RATE
POSTAGE & FEES PAID
NASA
Permit No. G-27

POSTMASTER: If Undeliverable (Section 158
Postal Manual) Do Not Return